

Effect of pre-deformation on aging characteristics and mechanical properties of Mg-Gd-Nd-Zr alloy

ZHENG Kai-yun(郑开云), DONG Jie(董杰), ZENG Xiao-qin(曾小勤), DING Wen-jiang(丁文江)

National Engineering Research Center of Light Alloys Net Forming, School of Materials Science and Engineering, Shanghai Jiao Tong University, Shanghai 200030, China

Received 15 July 2007; accepted 10 September 2007

Abstract: The effect of plastic deformation prior to artificial aging on the aging characteristics and mechanical properties of a Mg-11Gd-2Nd-0.5Zr (mass fraction, %) alloy was investigated. After solution treatment at 525 °C for 4 h, the alloy was subjected to cold stretching deformation of 0%, 5% and 10%, respectively. The as-deformed specimens possess high density of dislocations and mechanical twins, which increase with elevated deformation. As compared with non-stretched alloy, the stretched alloy shows accelerated age-hardening response and slightly enhanced peak hardness when aged at 200 °C. Comparison of the microstructures in undeformed and deformed specimens after 200 °C, 24 h aging reveals that pre-deformation induces the heterogeneous nucleation of precipitations at dislocations and twin boundaries in addition to the homogeneous precipitation in the matrix. Room and high temperature tensile test results show that pre-deformation enhances the strength of the alloy, especially at room temperature, though the ductility declines. The improvement in strength of deformed and aged alloy is attributed to the combined strengthening effect of precipitates, deformation structures and grain boundaries.

Key words: Mg-Gd-Nd-Zr alloy; pre-deformation; precipitation; microstructure; mechanical properties

1 Introduction

High performance magnesium-rare earth(RE) alloys have long been recognized as promising light structural materials for aerospace and automotive industries[1]. The strength of these alloys is achieved essentially via precipitation strengthening, and studies on microstructure under aged condition have shown the dispersive metastable precipitates present in the magnesium matrix[1–5]. In order to further improve the strength of the alloy, much work has been done to optimize the property and the structure of the precipitate phases in the alloys, especially by alloying. In the past two decades, considerable interest has been drawn to enhance the precipitation strengthening of Mg-RE alloys through alloying with a combination of two or more kinds of RE elements. This led to the successful design of Mg-Y-Nd base WE alloy series in 1980's[2]. Recently, Mg-heavy RE base systems with minor addition of light RE element, e.g. Mg-Gd-Nd, Mg-Dy-Nd, Mg-Gd-Y, have been developed to achieve even higher strength and creep resistance[4–9]. Despite the variety of alloy

systems, little work has been carried out to find processing approaches to achieve improved precipitation hardening response in Mg-RE alloys. In Ref.[10], WE54 alloy was cold rolled after solution treatment, which accelerated precipitation hardening response by promoting the nucleation of β_1 (FCC) precipitates. Such a thermomechanical processing with pre-deformation between solution treatment and artificial aging is extensively used in aluminum alloys[11–14], but rarely in Mg alloys. Therefore, it should be meaningful to introduce pre-deformation practice into magnesium alloys, especially the newly developed high strength Mg-RE alloys, and to perform further study on the structure—property relationships. In the present work, pre-deformation by cold stretching was performed on T4-treated Mg-11Gd-2Nd-0.4Zr alloy, and the microstructure, aging characteristics, mechanical properties of deformed specimens were investigated by comparison with those of undeformed counterparts.

2 Experimental

The chemical composition of the investigated alloy

was Mg-11.4Gd-2.2Nd-0.45Zr (mass fraction, %). As-cast ingot was solution treated at 525 °C for 4 h and quenched into water at about 80 °C. Plates cut from the as-quenched ingot were machined to dimension of 2.2 mm×20 mm×130 mm and subjected to 5% and 10% plastic deformation by stretching at room temperature. Artificial aging was conducted at 200 °C in oil bath, and the Vickers hardness was measured with 49 N load and 30 s holding time. Tensile test were performed on a Zwick-20KN material test machine at a rate of 1 mm/min, and rectangular specimens with gauge dimensions of 2 mm×3.5 mm×15 mm were used.

Metallographic specimens were polished and etched in 4%(volume fraction) nital, and observed by an optical microscope (OM, LEICA MEF4M). Thin foils for transmission electron microscope (TEM, JEM 2000EX and HITACH 800H) observation were electropolished and ion beam thinned (Gatan Model 691), and were examined at an acceleration voltage of 200 kV.

3 Results and discussion

3.1 Age-hardening behavior

The age-hardening curves of as-quenched and as-deformed specimens are shown in Fig.1. The average hardness of as-quenched specimens is about HV74.5, which is raised to HV76.1 and HV80.0 by 5% and 10 % cold stretching deformation, respectively. During aging at 200 °C, the hardness of undeformed specimen increases gradually to a peak around HV117 at 64 h. As for specimens with cold deformation, the maximum hardness increases slightly in comparison with undeformed specimen though the aging time of hardness peak is shifted to 24–32 h. In overaging stage, the hardness of deformed specimen declines faster than that

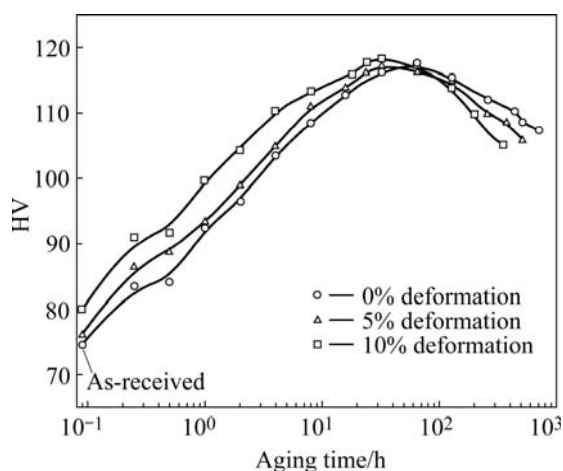


Fig.1 Age-hardening curves of specimens with 0, 5% and 10% pre-deformation at 200 °C

of undeformed one, indicating the promoted precipitation by strain.

3.2 Mechanical properties

The tensile properties of the alloy with and without deformation are listed in Table 1. It is noted that the strength of the alloy with 200 °C, 24 h aging increases with increasing pre-deformation ratio when the test temperature is below 250 °C; meanwhile, the elongation decreases with increasing deformation. In this case, the strengthening effect from aging is added by that from cold deformation. However, the alloy exhibits reverse tensile test result at 300 °C, i.e. the tensile strength of the pre-deformed specimens becomes lower than that of undeformed specimen. This phenomenon must be due to the more rapid overaging of the pre-deformed alloy at elevated temperature.

Table 1 Tensile properties of Mg-11Gd-2Nd-0.4Zr alloy

Condition	Temperature/ °C	$\sigma_{0.2}$ / MPa	σ_b / MPa	δ / %
	RT	222	336	2.5
Solution treatment+ 200 °C, 24 h aging	250	–	300	11.2
	300	–	251	12.9
Solution treatment+ 5% stretching+ 200 °C, 24 h aging	RT	276	351	2.0
	250	–	328	8.2
	300	–	250	14.6
Solution treatment+ 10% stretching+ 200 °C, 24 h aging	RT	298	381	1.4
	250	–	336	7.1
	300	–	247	15.2

3.3 Microstructures

Fig.2 shows the optical morphologies of the microstructures in as-quenched and as-deformed specimens. The as-quenched specimen exhibits a microstructure of polycrystalline α -Mg solid solution accompanied with some undissolvable particles. The average grain size of the specimen is 60 μ m. Due to the lack of active slip systems in Mg at low temperature, twinning is needed for grains in order to deform compatibly[15]. With stretching deformation of 5%, the alloy contains a noticeable density of twins that vary from grain to grain. The density of twins becomes more pronounced after the specimen is deformed by 10%. Fig.3 shows a pair of randomly found $\{10\bar{1}2\}$ twins with $[2\bar{1}\bar{1}0]_M // [2\bar{1}\bar{1}0]_T$ by TEM observation in the 10% cold stretched specimen. The dislocation structure in as-deformed specimens is recorded by TEM under two

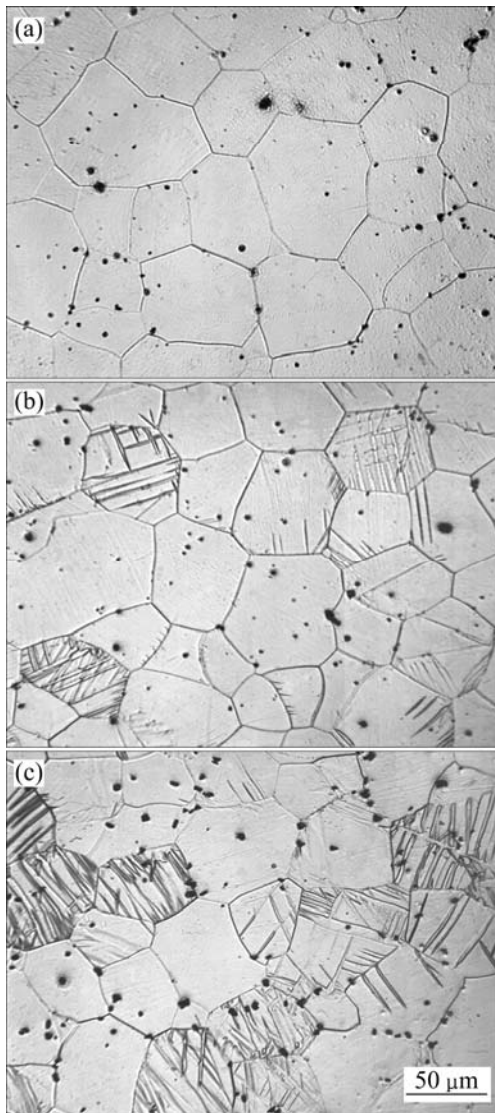


Fig.2 Optical images showing microstructure of as-quenched (a), 5% cold deformed (b) and 10% cold deformed (c) specimen

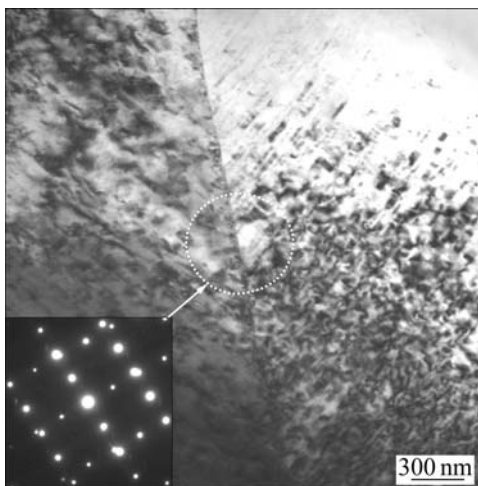


Fig.3 TEM image and SAED pattern of twins in 10% cold deformed specimen

beam condition with $g = \{01\bar{1}1\}_\alpha$ and $B = \langle 2\bar{1}\bar{1}0 \rangle_\alpha$. As can be seen from Fig.4, dislocations mostly lay on basal planes, indicating basal slip mechanism of deformation in solution treated specimen.

The TEM bright field images typical of the microstructure in undeformed and deformed specimens after aging at 200 °C for 24 h are shown in Fig.5. The images presented in Figs.5(a), (b) and (c) are viewed along $[0001]_\alpha$ axis, and those in Figs.5(d), (e) and (f) along $[2\bar{1}\bar{1}0]_\alpha$ axis. The distribution of precipitates in undeformed specimen after 200 °C, 24 h aging is shown in Figs.5(a) and (d). Under this near peak-aged condition, a very fine dispersion of β'' ($D0_{19}$) precipitates are present as thin platelets on $\{11\bar{2}0\}_\alpha$, extending along $\langle 1\bar{1}00 \rangle_\alpha$ directions, and small globular β' (BCO) particles located on β'' platelets, as seen from Fig.5(a). When observed along $[2\bar{1}\bar{1}0]_\alpha$ axis, the image shows only β' contrast (Fig.5(d)). The β'' platelets are approximately 25 nm in diameter and 3 nm in thickness, and the diameter of β' particles is not more than 5 nm. Compared with undeformed specimen, those specimens

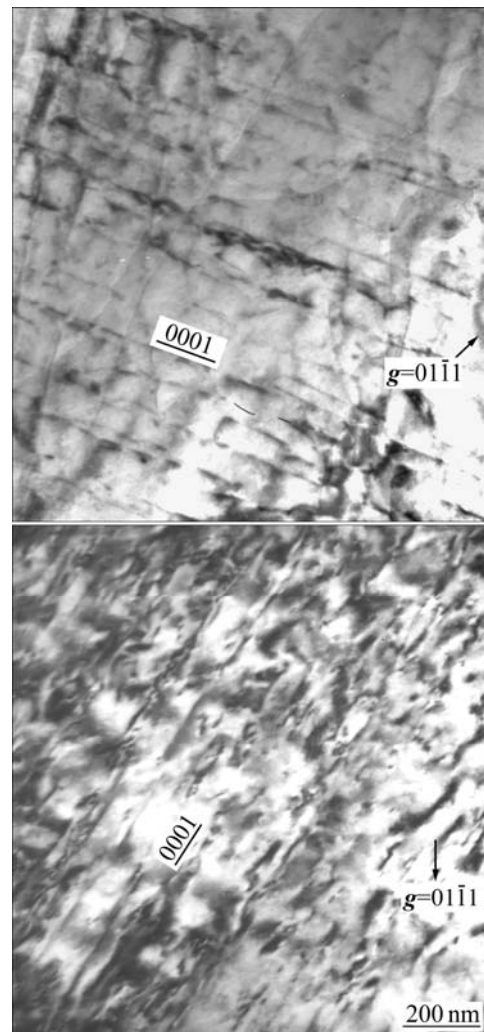


Fig.4 TEM images showing dislocation structure in 5% cold deformed (a) and 10% cold deformed (b) specimen

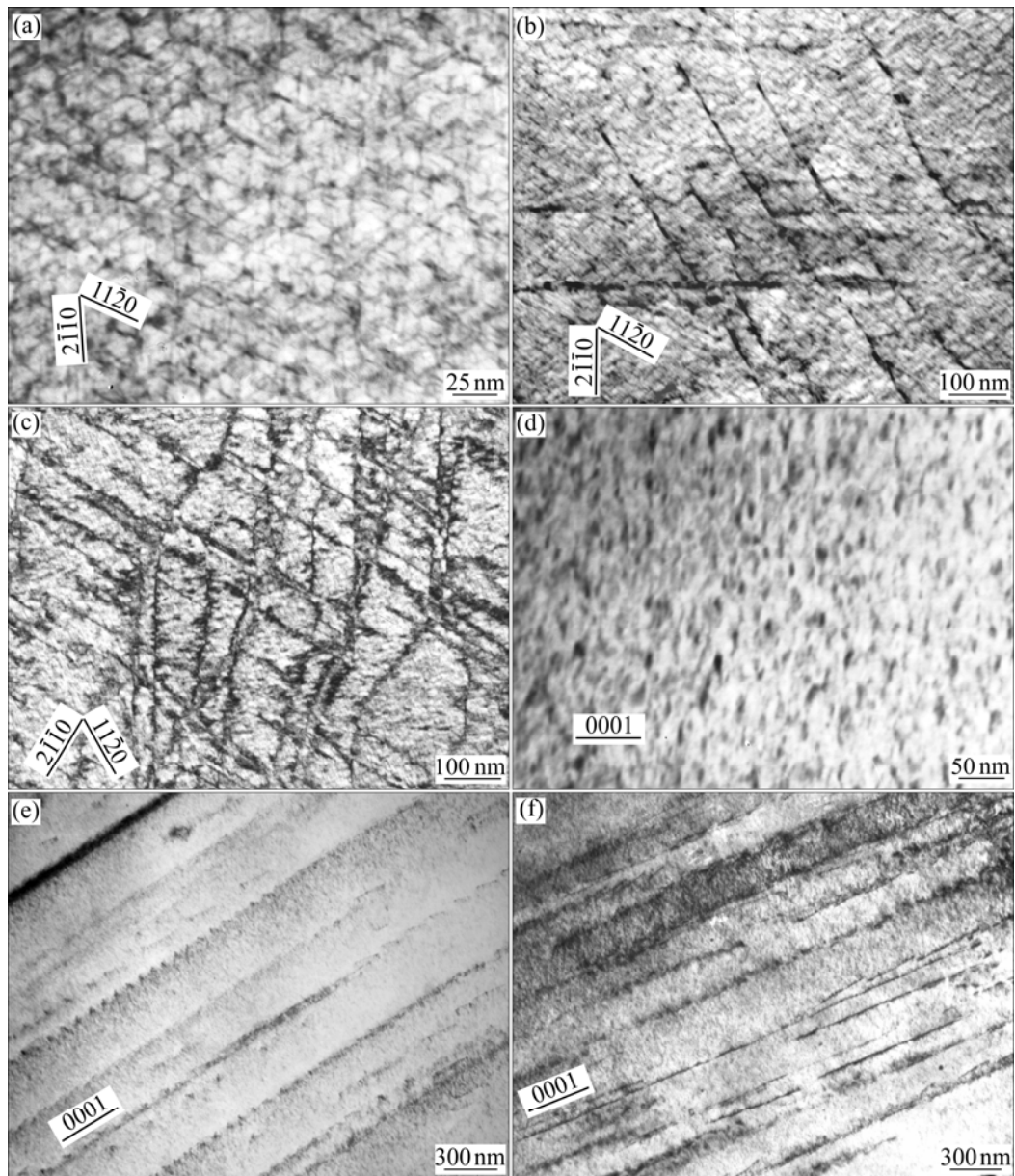


Fig.5 TEM images showing microstructure of 200 °C, 24 h aged specimens with 0 (a, d), 5% (b, e), 10% (c, f) pre-deformation: (a), (b) and (c) $B//[0001]_{\alpha}$; (d), (e) and (f) $B//[2\bar{1}\bar{1}0]_{\alpha}$

subjected to cold stretching and subsequent aging show a microstructure with heterogeneous nucleation of rod-shaped precipitates extending along $\langle 2\bar{1}\bar{1}0 \rangle_{\alpha}$ directions on dislocations, but the morphology of homogeneous precipitates in matrix is not so well-defined as undeformed specimen. This implies that the dislocations introduced by cold deformation promote the nucleation and growth of $\langle 2\bar{1}\bar{1}0 \rangle_{\alpha}$ rod-shaped precipitates and affect the formation of coherent β'' and β' precipitates. The accelerated aging-hardening kinetics might be induced by the heterogeneous precipitation of the rod-shaped phases. Given the experimental difficulty, the characterization of the rod-shaped precipitates was

not performed in the present study. Besides, coarse equilibrium phase is also found on twin boundaries. Fig.6 shows the superimposed selected area electron diffraction(SAED) pattern of β'' , β' precipitate and α -Mg matrix corresponding to Figs.5(a) and (b), respectively. Identical SAED patterns were also obtained in cold deformed specimens after 200 °C, 24 h aging. According to these microstructure analysis results, the improved strength of the pre-deformed and peak-aged specimens should be mainly attributed to the comprehensive contribution of precipitates, dislocation substructure with heterogeneous precipitates and grain/twin boundaries[16].

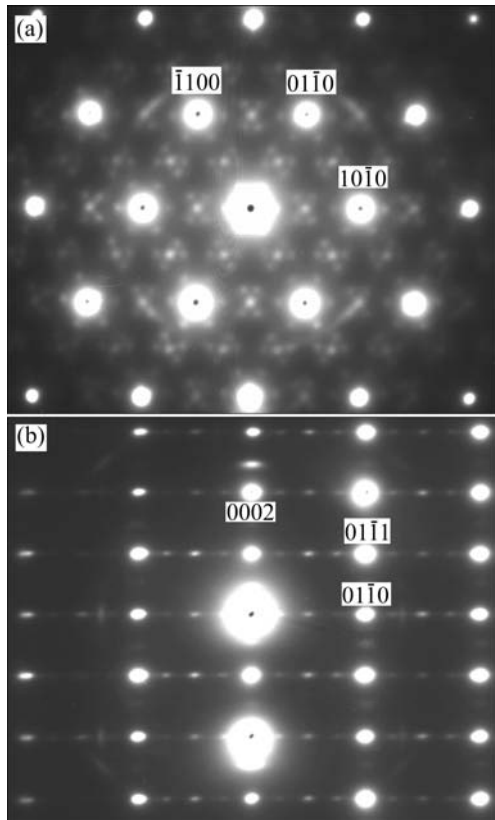


Fig.6 SAED patterns of 200 °C, 24 h aged specimen with $B // [0001]_{\alpha}$ (a) and $B // [2\bar{1}\bar{1}0]_{\alpha}$ (b)

4 Conclusions

1) Cold stretching deformation between solution treatment and aging at 200 °C creates high density of dislocations and twins, leading to acceleration in age-hardening response and small increase in peak hardness for Mg-11Gd-2Nd-0.4Zr alloy.

2) After 200 °C, 24 h aging, the microstructure of undeformed specimen contains a uniform and dense distribution of thin $\beta''(D0_{19})$ platelets decorated with globular $\beta'(BCO)$ particles, whereas that of pre-deformed specimen consists of not only β'' and β' precipitates distributing in the matrix but also $\langle 2\bar{1}\bar{1}0 \rangle_{\alpha}$ rod-shaped precipitates on dislocations.

3) With the strengthening of β'' and β' precipitate, dislocation substructure with heterogeneous precipitates and grain/twin boundaries, the cold deformed alloys

show remarkably improved strength on peak-aged condition especially at temperature below 250 °C.

References

- [1] MORDIKE B L. Creep-resistant magnesium alloys [J]. *Mater Sci Eng A*, 2002, 324(1/2): 103–112.
- [2] LORIMER G W, BAKER H. Structure–property relationships in cast magnesium alloys [C]// *Proceedings of London Conference on Magnesium Technology*. London, 1986: 47–53.
- [3] NIE J F, MUDDLE B C. Characterization of strengthening precipitate phases in a Mg-Y-Nd alloy [J]. *Acta Mater*, 2000, 50(7): 1691–1703.
- [4] APPS P J, KARIMZADEH H, KING J F, LORIMER G W. Precipitation reactions in magnesium-rare earth alloys containing yttrium, gadolinium or dysprosium [J]. *Scripta Mater*, 2003, 48(8): 1023–1028.
- [5] HE S M, ZENG X Q, PENG L M, GAO X, NIE J F, DING W J. Precipitation in a Mg-10Gd-3Y-0.4Zr (wt.%) alloy during isothermal ageing at 250 °C [J]. *J Alloys Compd*, 2006, 421(1/2): 309–313.
- [6] KAMADO S, KOJIMA Y, NINOMIYA R, KUBOTA K. Ageing characteristics and high temperature tensile properties of magnesium alloys containing heavy rare earth elements [C]// *Proceedings of the third International Magnesium Conference*. London, 1997: 327–342.
- [7] ANTHONY I, KAMADO S, KOJIMA Y. Aging characteristics and high temperature tensile properties of Mg-Gd-Y-Zr alloys [J]. *Mater Trans*, 2001, 42(7): 1206–1211.
- [8] ANTHONY I, KAMADO S, KOJIMA Y. Creep properties of Mg-Gd-Y-Zr alloys [J]. *Mater Trans*, 2001, 42(7): 1212–1218.
- [9] ZHENG K Y, DONG J, ZENG X Q, DING W J. Effect of thermo-mechanical treatment on the microstructure and mechanical properties of a Mg-6Gd-2Nd-0.5Zr alloy [J]. *Mater Sci Eng A*, 2007, 454/455(1/2): 314–321.
- [10] HILDITCH T, NIE J F, MUDDLE B C. The effect of cold work on precipitation in alloy WE54 [C]// *Proceedings of Magnesium Alloys and Their Applications*. Frankfurt, 1998: 339–344.
- [11] RINGER S P, MUDDLE B C, POLMEAR I J. Effect of cold work on precipitation in Al-Cu-Mg-(Ag) and Al-Cu-Li-(Mg-Ag) alloys [J]. *Metall Trans A*, 1995, 26(7): 1659–1667.
- [12] HAMANA D, BOUCHEAR M, DERAFA A. Effect of plastic deformation on the formation and dissolution of transition phases in Al-12wt.% Mg alloy [J]. *Mater Chem Phys*, 1998, 57(2): 99–110.
- [13] ÜNLÜ N, GABLE B M, SHIFLET G J, STARKE E A. The effect of cold work on the precipitation of Ω and θ' in a ternary Al-Cu-Mg alloy [J]. *Metall Trans A*, 2003, 34(12): 2757–2768.
- [14] LIANG W J, PAN Q L, HE Y B, ZHU Z M, LIU Y F. Effect of predeformation on microstructure and mechanical properties of Al-Cu-Li-Zr alloy containing Sc [J]. *Mater Sci Tech*, 2007, 23(4): 395–399.
- [15] YOO M H. Slip, twinning, and fracture in hexagonal close-packed metals [J]. *Metall Trans A*, 1981, 12(3): 409–418.
- [16] KELLY A, NICHOLSON R B. *Strengthening methods in crystals* [M]. London: Elsevier Publishers, 1971.

(Edited by YANG Bing)